Preprints,18th IFAC Symposium on System Identification
July 9-11, 2018. Stockholm, Sweden

Inverse System Estimation for Feedforward: A Kernel-Based Approach for Non-Causal Systems

Lennart Blanken * **Ids van den Meijdenberg** * **Tom Oomen** *

* *Eindhoven University of Technology, Department of Mechanical Engineering, Eindhoven, The Netherlands (l.l.g.blanken@tue.nl)*

Abstract: Accurate models of inverse systems are required for high performance in inverse model-based feedforward control. Identification of inverse systems can be challenging, especially if the inverse system has poles outside the typical stability region. The aim of this paper is to estimate non-causal models of inverse systems, for intended use in feedforward control, where non-causality can be exploited to compensate 'unstable' poles. The developed method employs kernel-based regularization to improve the bias/variance trade-off, where the non-causal kernel is constructed using rational basis functions that include poles outside the usual stability region. The benefits of the developed method are demonstrated on an example, including non-causality.

Keywords: Identification; feedforward control; inverse system; non-causality; regularization

1. INTRODUCTION

Accurate models of inverse systems are often required for high control performance in inverse model-based feedforward control (Boeren et al., 2015; Butterworth et al., 2012; Van Zundert and Oomen, 2017). Indeed, known disturbances can effectively be rejected, or tracked, before these affect the system by using an inverse model in series with the original system. The aim of the present paper is to estimate models of inverse systems based on measured data, see, e.g., Jung and Enqvist (2013) for the causal case.

Identification of inverse systems leads to additional challenges in certain situations, including if the forward system is i) non-minimum phase (NMP), and ii) non-square, i.e., has a different number of inputs than outputs (van Zundert and Oomen, 2017). This paper focuses on the first aspect, i.e., systems with zeros outside the unit disc. Indeed, then the inverse system has poles outside the typical stability region, i.e., the unit disc, which would result in unbounded impulse responses in a typical classical interpretation.

An essential aspect in system identification, hence also in identification of inverse models, is model order selection. This has recently attracted renewed interest, in particular through developments of regularized system identification in the Gaussian process regression (GPR) framework (Rasmussen and Williams, 2006; Pillonetto and Nicolao, 2010; Chen et al., 2012). Regularization techniques have been shown to substantially improve the bias/variance trade-off, as encountered in traditional maximum likelihood/prediction error methods (ML/PEM) (Ljung, 1999; Söderström and Stoica, 1989). In particular, in the GPR framework, the impulse response is assumed to be a realization of a zero-mean Gaussian process with a certain covariance function, called a kernel. The kernel imposes priors on the system dynamics, including resonant dynamics (Chen and Ljung, 2015; Darwish et al., 2018), smoothness, and stability aspects, e.g., decay of the impulse response (Pillonetto and Nicolao, 2010; Chen et al., 2012).

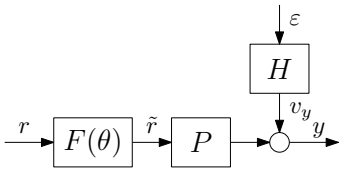

Fig. 1. Inverse-model based feedforward: high tracking performance ($y \approx r$) requires inverse model $F = P^{-1}$.

Although recent developments in kernel-based regularized identification techniques are promising, their advantages can not yet be fully exploited in identification of inverse systems, due to the presence of poles outside the stability region. The aim of this paper is to develop a kernel-based regularized identification approach for finite impulse response (FIR) models of inverse systems, for intended use in feedforward control. Whereas (inverse) systems with poles outside the unit disc are typically interpreted as unstable, causal, operators on $\mathcal{L}_2$, in feedforward control such systems can be interpreted as non-causal operators on $\mathcal{L}_2$ with bounded impulse response. The developed kernel is constructed using *non-causal* rational orthonormal basis functions in $\mathcal{L}_2$ (Blanken et al., 2018) to impose a prior on non-causality of the inverse system. This extends earlier *causal* kernels, including the diagonal/correlated (DC) kernel (Chen et al., 2012), and kernels (Chen and Ljung, 2015; Darwish et al., 2018) based on causal rational orthonormal basis functions in $\mathcal{H}_2$ (Ninness and Gustafsson, 1997; Heuberger et al., 2005). Benefits of the developed approach are demonstrated on an NMP system.

[1] This work is supported by Océ Technologies, and is part of the research programme VIDI with project number 15698, which is (partly) financed by the Netherlands Organisation for Scientific Research (NWO).

Notation: All systems are discrete-time, single-input single-output, and linear time-invariant. The complex indeterminate $z \in \mathbb{C}$ is tacitly omitted when it is clear from the context. The following standard notation is used, see, e.g., Heuberger et al. (2005). Let $\mathbb{D}$ denote the open unit disc: $\{z, |z| < 1\}$, $\mathbb{T}$ the unit circle: $\{z, |z| = 1\}$, and $\mathbb{E}$ the complement of the closed unit disc: $\{z, |z| > 1\}$. $\mathcal{L}_2$ denotes the set of complex functions that are square integrable on $\mathbb{T}$. $\mathcal{H}_2$ denotes the set of complex functions that are square integrable on $\mathbb{T}$ and analytic for $|z| \geq 1$. The space $\mathcal{H}_{2-}$ denotes all functions in $\mathcal{H}_2$ that are zero at infinity, such as strictly causal systems, and $\mathcal{H}_{2-}^{\perp} = \mathcal{L}_2 \setminus \mathcal{H}_{2-}$. The prefix $\mathcal{R}(\cdot)$ denotes the real rational subspace of $(\cdot)$. $\mathbb{R}[z^{-1}]$ denotes the polynomial ring in indeterminate z^{-1} with coefficients in $\mathbb{R}$, and $\mathbb{R}[z, z^{-1}]$ denotes the Laurent polynomial ring in indeterminate z with coefficients in $\mathbb{R}$. Laurent polynomials include both positive and negative exponents of the indeterminate. $\overline{\mathbb{E}}$ denotes mathematical expectation. Signals are often tacitly assumed to be of length N. The two-norm of a vector $x \in \mathbb{R}^N$ is given by $\|x\|_2 = \sqrt{x^\top x}$. A is positive definite if $x^\top Ax > 0$, $\forall x \neq 0$.

2. PROBLEM FORMULATION

2.1 Inverse-Model Based Feedforward Configuration

Consider the control configuration shown in Figure 1, where the true, unknown system is denoted $P(z)$, and the feedforward controller $F(z)$ is connected in series. Let $r(t)$ denote an a priori known finite time reference signal with $t = 1, \ldots, N$, $y(t)$ the output signal, $v_y(t) = H(q)\varepsilon(t)$ an unknown disturbance with H monic and $\varepsilon(t)$ an i.i.d. zero-mean normally distributed noise sequence with variance σ^2, uncorrelated with $r(t)$, and $\tilde{r}(t)$ the feedforward signal. The tracking error $e = r - y$ is given by

$$e(t) = (1 - P(q)F(q))\, r(t) - H(q)\varepsilon(t),$$

where it is assumed that P is stable, and is described by the rational representation with causal impulse response

$$P(q) = \frac{B_0(q)}{A_0(q)} = \sum_{k=0}^{\infty} p_k q^{-k},$$

with $B_0(q), A_0(q) \in \mathbb{R}[q^{-1}]$. Optimal tracking performance, i.e., $\overline{\mathbb{E}}e(t) = 0$, $\forall r \neq 0$ is achieved if $F(z) = P^{-1}(z)$. Clearly, the inverse system $P^{-1}(z)$ is unknown.

Remark 1. *If P is unstable, the system can be stabilized using feedback control, and the feedforward can be connected in series with the closed-loop $\tilde{P} = (I+PC)^{-1}PC$. Note that the zeros of P form a subset of the zeros of $\tilde{P}$.*

2.2 Identification of Inverse System

Inverse model-based feedforward requires a parametric model of the inverse system P^{-1}. Such models may be obtained through, e.g., first principles modeling, or identified based on measured data, e.g., input data $r(t)$ and output data $y(t)$. Essentially, two approaches can be distinguished to estimate models of P^{-1} based on data $\{r(t), y(t)\}_{t=1}^{N}$:

- A forward model $\hat{P}(\theta)$ is estimated using input $r(t)$ and output $y(t)$, which is subsequently inverted to obtain $\hat{P}^{-1}(\theta)$, see, e.g., Butterworth et al. (2012); Van Zundert and Oomen (2017) for overviews.

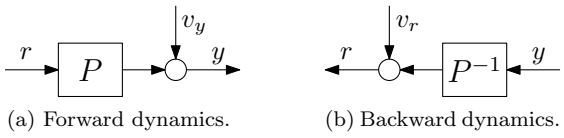

(a) Forward dynamics. (b) Backward dynamics.

Fig. 2. Forward and backward identification setting.

- An inverse, or backward, model $\widehat{P^{-1}}(\theta)$ is estimated directly using *input* $y(t)$ and *output* $r(t)$, see, e.g., Jung and Enqvist (2013); Boeren et al. (2015).

The aim of this work is to identify P^{-1} directly, i.e., the latter approach. Potential advantages are i) the inverse model is estimated in the setting it is going to be used in (Gevers, 2005), see also Boeren et al. (2015) for a feedforward perspective, and ii) no inversion step is required. Essentially, the approach corresponds to identification of parametric model $F = \widehat{P^{-1}}$, given *input* data $y(t)$ and *output* data $r(t)$ from the data generating system

$$r(t) = P^{-1}(q)y(t) + v_r(t),$$

where $v_r(t) = -P^{-1}(q)H(q)\varepsilon(t)$. This interpretation of the system is schematically depicted in Figure 2.

Remark 2. *In the backward setting, the additive 'output' noise $v_r(t)$ is a filtered version of $v_y(t)$, i.e., $v_r(t) = -P^{-1}(q)H(q)\varepsilon(t)$. In view of length limitations, here it is assumed that $P^{-1}H = 1$, i.e., $v_r(t)$ is an i.i.d. zero-mean normally distributed noise sequence with variance σ^2. This assumption can be relaxed by appropriately accounting for the noise colouring, see, e.g., Van den Meijdenberg (2017).*

Important aspects in inverse system identification include stability and causality of the inverse model, and selection of the model structure and order. Indeed, if $P(z)$ has NMP dynamics, i.e., zeros in $\mathbb{E}$, then $P^{-1}(z)$ has poles outside of the usual stability region $\mathbb{D}$. To anticipate on Section 3, this can effectively be dealt with in feedforward, where non-causality can be exploited to determine exact inverses with bounded responses, even with poles outside of $\mathbb{D}$.

2.3 Regression Formulation of Inverse Model Identification

The following general structure for the model F of $\widehat{P^{-1}}$ is used, that allows for non-causal models:

$$F(q, \theta) = \sum_{k=-n_{ac}}^{n_c} \theta_k q^{-k} = \Psi(q)\theta, \tag{1}$$

where $\theta \in \mathbb{R}^{n_c+n_{ac}+1}$, n_c is the number of strictly causal terms, n_{ac} the number of anti-causal terms, and the basis functions $\Psi(q) = [q^{n_{ac}}, q^{n_{ac}-1}, \ldots, q^0, \ldots, q^{-n_c}]$ are Laurent polynomials, i.e., $q^{-k} \in \mathbb{R}[q, q^{-1}]$, as often used in feedforward control, see, e.g., Boeren et al. (2015). This is a generalization of the widely used FIR models in system identification (Ljung, 1999; Pillonetto et al., 2014; Chen and Ljung, 2015), yet allows for non-causal models. The estimation problem is written as a linear regression model

$$r_N = \Phi_N\theta + v_N, \tag{2}$$

where $r_N \in \mathbb{R}^N$ is the data, $\Phi_N = \Psi(q)y(t) \in \mathbb{R}^{N\times(n_{ac}+1+n_c)}$ is the regression matrix, and v_N is the i.i.d. normally distributed noise with distribution $\mathcal{N}(0, \sigma^2 I_N)$.

For a given model structure, e.g., (1), in the ML/PEM framework the estimate $\hat{\theta}$ is determined according to

$$\hat{\theta}_{LS} = \arg\min_{\theta} \|r_N - \Phi_N\theta\|_2^2 \quad (3)$$
$$= \left(\Phi_N^\top \Phi_N\right)^{-1} \Phi_N^\top r_N.$$

Assuming that $F(q,\theta)$ contains P^{-1}, the estimator (3) is asymptotically efficient, i.e., as $N \to \infty$ the covariance matrix of $\hat{\theta}_{LS}$ approaches the Cramér-Rao limit. However for short data records, ML/PEM methods may suffer from high variance induced by the stochastic noise v_N, see, e.g., Pillonetto et al. (2014). To handle this, typically i) the model order is trimmed using, e.g., AIC or cross-validation (Ljung, 1999; Söderström and Stoica, 1989), or ii) compact model structures are employed, e.g., rational models as in (Blanken et al., 2018; Bolder et al., 2015) for feedforward. Alternatively, recent developments in identification aim to optimize the bias/variance by kernel-based regularization. Although these results are promising, their advantages can not yet be employed for estimation of non-causal models.

2.4 Contributions

The main contribution is a kernel-based regularized identification approach for non-causal FIR models of inverse systems, with attention to stability and non-causality. The following subcontributions are distinguished:

i. the role of non-causality is investigated in view of inverse system identification for feedforward;
ii. an example non-causal kernel is built using non-causal rational orthonormal basis functions that have shown to be suitable for traditional identification of inverse systems (Blanken et al., 2018);
iii. the benefits of the presented method for inverse-model based feedforward control are demonstrated.

3. STABILITY & CAUSALITY OF INVERSE SYSTEM

If $P(z)$ has zeros in $\mathbb{E}$, then $P^{-1}(z)$ has poles in $\mathbb{E}$. In system identification, systems with poles in $\mathbb{E}$ are often interpreted as unstable, i.e., with unbounded causal impulse response, see, e.g., Ljung (1999). For feedforward control however, this need not be the case, since non-causal filtering operations are allowed with a priori known signal r. This allows to interpret systems with poles in $\mathbb{E}$ as non-causal, with non-causal and bounded impulse response. See, e.g., Zhou et al. (1996, Definition 4.3) for this duality of interpretation. Next, this latter interpretation is utilized for feedforward control. The relevance of the approach is illustrated using an example. It is assumed that $P^{-1} \in \mathcal{L}_2$, i.e., P has no zeros on $\mathbb{T}$. For inverse systems with non-hyperbolic dynamics, i.e., poles on $\mathbb{T}$, see Devasia (1999).

By interpreting P^{-1} as a non-causal and bounded operator on $\mathcal{RL}_2$, see, e.g., Vinnicombe (2001, Section 1.5) for a concise example in the context of feedback control, the bilateral (two-sided) Z-transform, denoted $\mathcal{Z}\{\cdot\}$, gives

$$P^{-1}(z) = \frac{A_0(z)}{B_0(z)} = \mathcal{Z}\{\theta_k^o\} = \sum_{k=-\infty}^{\infty} \theta_k^o z^{-k}, \quad (4)$$

where the sum converges in a strip that includes the unit circle since $P^{-1}(z) \in \mathcal{L}_2$. The non-causal $\{\theta_k^o\}$ arises from solving the underlying difference equation also for negative time, typically with boundary conditions of zero at $\pm\infty$.

The bounded response in (4) allows to uniquely compute non-causal feedforward signals. This is done by the split $P^{-1}(z) = [P^{-1}]_+(z) + [P^{-1}]_-(z)$, where

$$[P^{-1}]_+(z) = \sum_{k=1}^{\infty} \theta_k^o z^{-k}, \quad [P^{-1}]_-(z) = \sum_{k=-\infty}^{0} \theta_k^o z^{-k}. \quad (5)$$

The strictly causal part $[P^{-1}]_+(z) \in \mathcal{RH}_{2-}$ has all poles in $\mathbb{D}$; the non-causal part $[P^{-1}]_-(z) \in \mathcal{RH}_{2-}^{\perp}$ has all poles in $\mathbb{E}$ (Söderström, 2002, Lemma 7.1). To anticipate on results in Section 5, here it is chosen to include the feedthrough θ_0^o in $[P^{-1}]_-(z)$, i.e., in $\mathcal{RH}_{2-}^{\perp}$, although it is also part of $\mathcal{H}_2$ for discrete-time systems, see, e.g., Chen and Francis (1995, Example 4.5.5). State-space expressions for the split (5) are provided by, e.g., Van Zundert and Oomen (2017).

The feedforward signal $\tilde{r}(t) = P^{-1}(q)r(t)$, see Figure 1, can then be computed by filtering the causal $[P^{-1}]_+(z)$ forwards in time with $r(t)$, and filtering the non-causal $[P^{-1}]_-(z)$ with *a priori known* $r(t)$ backwards in time.

Remark 3. *The backwards filtering operation can be implemented forwards in time by filtering the adjoint system $[P^{-1}]_-^*(z) = [P^{-1}]_-(\frac{1}{z})$ with the time-reversed input signal, see Bolder et al. (2016).*

Remark 4. *The presented non-causal approach closely resembles spectral methods, including Wiener filtering, see, e.g., Söderström (2002, Section 7.3), where the optimal (unrealizable) Wiener filter is non-causal, and the optimal causal (realizable) Wiener filter is built using an adjoint.*

Remark 5. *Exact feedforward, $F(z) = P^{-1}(z)$, requires infinite non-causal control, see* (4)*. In practice, a trade-off exists between finite preview time and non-exact tracking, see Middleton et al. (2004); Van Zundert et al. (2016).*

Next, the non-causal interpretation of inverse systems for feedforward, see (4), is illustrated using an example.

Example 6. *Consider the non-minimum phase system $P(z) = \frac{z-2}{z}$, with input $r(t) = (\frac{1}{2})^t$ for $t \geq 0$, and $r(t) = 0$ for $t < 0$, hence $R(z) = \frac{z}{z-0.5}$. The optimal feedforward is given by $\tilde{R}(z) = P^{-1}(z)R(z) = \frac{4z}{3(z-2)} - \frac{z}{3(z-0.5)}$. Now, note that $\tilde{R}(z)$ can be interpreted in two ways:*

- *Applying the inverse unilateral Z-transform to $\tilde{R}(z)$ gives $\tilde{r}(t) = \frac{4}{3}2^t - \frac{1}{3}(\frac{1}{2})^t$ for $t \geq 0$, and $\tilde{r}(t) = 0$ for $t < 0$, which is causal and unbounded.*
- *Applying the inverse bilateral Z-transform gives $\tilde{r}(t) = -\frac{4}{3}2^t$ for $t < 0$, and $\tilde{r}(t) = -\frac{1}{3}(\frac{1}{2})^t$ for $t \geq 0$, which is non-causal and bounded.*

The relevant signals are shown in Figure 3. It is observed that although both interpretations give perfect tracking, i.e., $y(t) = P(q)\tilde{r}(t) = r(t)$, the causal feedforward grows unbounded, whereas the non-causal signal is bounded.

4. A KERNEL-BASED REGULARIZATION APPROACH FOR NON-CAUSAL FIR ESTIMATION

A kernel-based regression approach is developed to estimate non-causal inverse models for feedforward control.

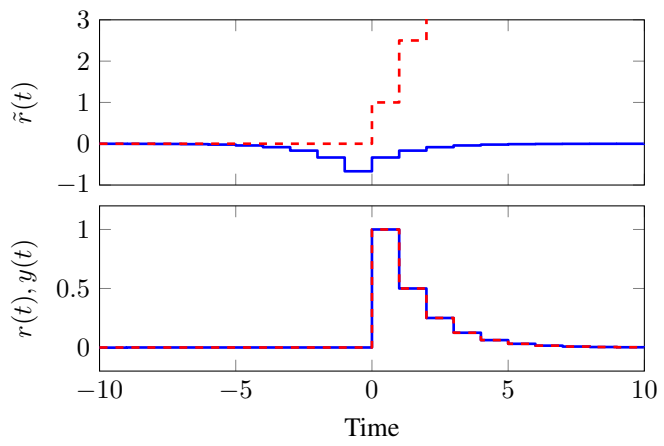

Fig. 3. Although both the non-causal (—) and causal interpretations (– –) enable perfect tracking (bottom), the causal feedforward signal grows unbounded (top), while the non-causal signal remains bounded.

The approach builds on kernel-based identification techniques, see, e.g., Pillonetto et al. (2014), yet focuses on estimating non-causal inverse models. Whereas typically in system identification the kernel is used to impose stability aspects, here it is used to encode non-causality.

4.1 Regularized Least Squares

Given model (2), the regularized least squares problem is:

$$\hat{\theta}_{ReLS} = \arg\min_{\theta} \|r_N - \Phi_N\theta\|_2^2 + \sigma^2\theta^\top D^{-1}(\alpha)\theta \quad (6)$$

$$= \left(D(\alpha)\Phi_N^\top\Phi_N + \sigma^2 I_N\right)^{-1} D(\alpha)\Phi_N^\top r_N, \quad (7)$$

where $D(\alpha) \succeq 0$ has the interpretation of regularization matrix, or kernel matrix, and α are design variables, typically referred to as hyperparameters. In case $D(\alpha)$ is singular, (6) should be interpreted as in Pillonetto et al. (2014, Remark 1). Since for the considered model (1), D regularizes parameters θ corresponding to both anti-causal and causal terms, it is referred to as a non-causal kernel.

Remark 7. (6) *can be interpreted in a Bayesian setting, see, e.g., Chen et al. (2012). Here, θ is assumed a random variable of Gaussian distribution with zero mean and covariance D, which forms the prior. With $v_r(t)$ independently Gaussian distributed as $v_r(t) \sim \mathcal{N}(0, \sigma^2)$, r_N and θ will be jointly Gaussian variables with prior distribution*

$$\begin{bmatrix}\theta \\ r_N\end{bmatrix} \sim \mathcal{N}\left(\begin{bmatrix}0\\0\end{bmatrix}, \begin{bmatrix}D & D\Phi_N^\top \\ \Phi_N D & \Phi_N D\Phi^\top + \sigma^2 I_N\end{bmatrix}\right).$$

Given the data r_N, the posterior distribution of θ is $\theta|r_N \sim \mathcal{N}(\hat{\theta}_{ReLS}, D^{post})$ with mean $\hat{\theta}_{ReLS}$ given by (7), and covariance D^{post}.

4.2 Role of Regularization Matrix

The regularization matrix D balances adherence to measured data and the imposed prior on θ. A carefully chosen D enables to decrease the variance of $\hat{\theta}$, at the price of introducing some bias with respect to 'true' parameters θ^o, see (4). In fact, Chen et al. (2012, Theorem 1) show that the optimal regularization matrix, with respect to minimization of the mean square error (MSE) matrix of $\hat{\theta} - \theta^o$, exists and is given by $D^{opt} = \theta^o\theta^{o\top}$. Although D^{opt} is unknown, it provides a design guideline: expected dynamical properties of the system can be imposed in D.

For identification of inverse systems for feedforward control, relevant prior expectations include non-causality, see Section 3, resonant dynamics, i.e., complex pole pairs, and exponential decay of the impulse response, both for positive and negative time. In the next section, a suitable parametric structure for a non-causal kernel is developed.

5. A NON-CAUSAL KERNEL BASED ON OBFS IN $\mathcal{L}_2$

In this section, a non-causal parametric kernel is developed that is suitable for non-causal inverse model estimation. The kernel is constructed using non-causal rational orthonormal basis functions in $\mathcal{RL}_2$, see, e.g., Blanken et al. (2018), to allow lightly damped and non-causal responses. This is in contrast with causal kernels (Chen and Ljung, 2015; Darwish et al., 2018) which are based on causal rational orthonormal basis functions in $\mathcal{RH}_{2-}$, see, e.g., Ninness and Gustafsson (1997); Heuberger et al. (2005).

5.1 Non-Causal Orthonormal Basis Functions in $\mathcal{L}_2$

A construction method is presented for non-causal rational orthonormal basis functions, which are used to construct the non-causal kernel in Subsection 5.2. The orthonormality is with respect to the standard inner product on $\mathcal{L}_2$:

$$\frac{1}{2\pi}\int_{-\pi}^{\pi} \psi_k(e^{i\omega})\psi_l(e^{-i\omega})d\omega = \delta_{k,l} = \begin{cases}1 & \text{if } k = l,\\ 0 & \text{if } k \neq l.\end{cases}$$

The considered orthonormal basis functions are defined by the sequences $\xi_s = \{\xi_{s,k}\}_{k=1,2,\ldots}$ and $\xi_u = \{\xi_{u,k}\}_{k=0,-1,\ldots}$, with $\xi_{s,k}, \xi_{u,k} \in \mathbb{D}$, $\forall k$, which define the poles of the rational basis functions. The basis functions are given by

$$\psi_k(z) = \begin{cases}\dfrac{\sqrt{1-|\xi_{s,k}|^2}}{z-\xi_{s,k}}\phi_k(z,\xi_s), & \text{if } k > 0,\\ \dfrac{\sqrt{1-|\xi_{u,k}|^2}}{1-\overline{\xi_{u,k}}z}\phi'_k(z,\xi_u), & \text{if } k \leq 0,\end{cases} \quad (8)$$

where the all-pass transfer functions ϕ_k, ϕ'_k are defined by

$$\phi_k(z,\xi) = \begin{cases}1 & \text{if } k = 1,\\ \displaystyle\prod_{m=1}^{k-1}\frac{1-\overline{\xi_m}z}{z-\xi_m} & \text{if } k > 1.\end{cases}$$

$$\phi'_k(z,\xi) = \begin{cases}1 & \text{if } k = 0,\\ \displaystyle\prod_{m=1}^{k-1}\frac{z-\xi_m}{1-\overline{\xi_m}z} & \text{if } k < 0.\end{cases}$$

The sequence $\{\psi_k\}_{k>0} \subseteq \mathcal{H}_{2-}$ forms the well-known Takenaka-Malmquist functions, and consists of strictly causal functions. The set $\{\psi_k\}_{k\leq 0} \subseteq \mathcal{H}_{2-}^{\perp}$ contains anti-causal functions and direct feedthrough terms, e.g., select $\xi_{u,0} = 0$. To ensure real-valued responses, the complex poles ξ_s, ξ_u should occur in complex conjugate pairs.

5.2 Non-Causal Kernels Based on Orthonormal Functions

The basis functions $\{\psi_k(e^{i\omega})\}$ in (8) are transformed to the time domain through the (inverse) Fourier transform:

$$\psi_k(e^{i\omega}) = \mathcal{F}\{\varphi_k(t)\}, \quad \varphi_k(t) = \mathcal{F}^{-1}\{\psi_k(e^{i\omega})\},$$

where $\mathcal{F}\{\varphi_l(t)\}$ is defined as $\psi_l(e^{i\omega}) = \sum_{k=-\infty}^{\infty} \varphi_l(k) z^{-k}$. Since $\{\psi_k(z)\}$ forms an orthonormal basis in the Hilbert space $\mathcal{L}_2$, the time-domain responses $\{\varphi_k(t)\}$ form an orthonormal basis in $\ell_2(-\infty, \infty)$ in the sense that

$$\sum_{t=-\infty}^{\infty} \varphi_k(t)\varphi_l^*(t) = \delta_{k,l} = \begin{cases} 1 & \text{if } k = l, \\ 0 & \text{if } k \neq l. \end{cases} \tag{9}$$

It can be shown, see Ninness et al. (1999) for the causal case, that the space spanned by $\{\varphi_k(t)\}_{k=-n_u}^{n_s}$, denoted $\mathcal{H}_D$ in the sequel, equipped with inner product as in (9) is a reproducing kernel Hilbert space with reproducing kernel

$$D(t, t') = \sum_{k=-n_u}^{n_s} \varphi_k(t)\varphi_k^*(t') = \Psi(t)\Psi^*(t'), \tag{10}$$

where $\Psi(t) = [\varphi_{n_{ac}}(t), \varphi_{n_{ac-1}}(t), \ldots, \varphi_0(t), \ldots, \varphi_{n_c}(t)]$. That is, the kernel D induces the space $\mathcal{H}_D$ in which the impulse response to be estimated is hypothesized to lie.

In contrast with pre-existing causal kernel structures, see, e.g., Chen and Ljung (2015); Pillonetto et al. (2014), the time indices t, t' in (10) take both positive and negative values: $-n_{ac} \leq t \leq n_c$, reflecting non-causality. This is key for modeling inverse systems with poles in $\mathbb{E}$, see Section 3.

5.3 Hyperparameter Selection

The design variables α, see (6), of the kernel (10) are the poles of basis functions (8). In view of $D^{opt} = \theta^o\theta^{o\top}$, α should be chosen close to the true poles of P^{-1}.

Several approaches can be taken to select the hyperparameters. For instance, they can be estimated using an empirical Bayes approach by maximizing the marginal likelihood with respect to data, see, e.g., Pillonetto and Chiuso (2015); Darwish et al. (2018). They may also be chosen based on expectations on the zeros of P, e.g., obtained from frequency response function measurements.

6. EXAMPLE

In this section, the developed approach for inverse-model estimation for feedforward control is validated on an example system, with attention to the effects of non-causality and bias/variance on feedforward performance. The forward system is $P(z) = \frac{GC}{1+GC}$, see Remark 1, with

$$G(z) = \frac{4.0564 \times 10^{-4}(z^2 - 1.963z + 0.9704)(z^2 - 2.007z + 1.041)}{(z-1)^2(z^2 - 1.927z + 0.9418)(z^2 - 1.893z + 0.9418)},$$

and feedback controller $C(z) = \frac{59.073(z-0.9834)}{(z-0.8597)}$. $P(z)$ has lightly damped zeros at $1.003 \pm 0.184i$, $0.982 \pm 0.0839i$ and 0.983, i.e., the inverse system $P^{-1}(z)$ has two poles in $\mathbb{E}$.

Three estimation methods for non-causal models $F(\theta)$ of P^{-1} are compared, see (1), each with $n_{ac} = n_c = 300$:

- the non-regularized least-squares estimator (3).
- the developed kernel-based estimator (6) with non-causal kernel as in (10), where the poles are chosen as $\xi_s = \{0.985 \pm 0.1i, 0.985\}$ and $\xi_u = \{1.003 \pm 0.2i\}$.
- the developed kernel-based estimator (6) with the pre-existing *causal* kernel as in (10), where the poles are chosen as $\xi_s = \{0.985 \pm 0.1i, 0.985\}$ and $\xi_u = \emptyset$. That is, the causal terms in (1) are regularized, whereas the non-causal are not regularized.

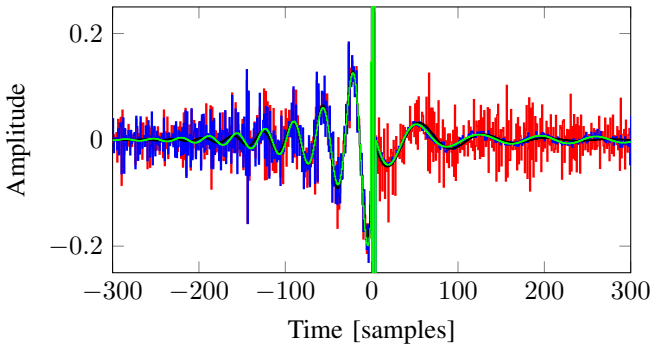

Fig. 4. Estimates $\hat{\theta}$ from single realization: the non-regularized estimate (—) indicates high variance, whereas using the developed *non-causal* kernel (—) significantly improves accuracy w.r.t. the true impulse response of P^{-1} (—). Using a pre-existing *causal* kernel (—), only the causal terms ($t \geq 0$) are regularized.

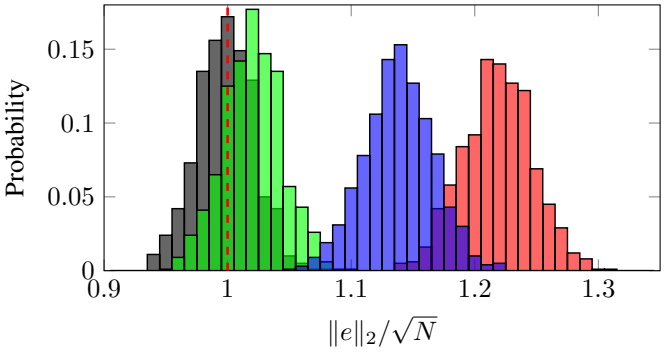

Fig. 5. Monte Carlo simulations: feedforward performance $\|e\|_2$ with estimated non-causal inverse models. The developed non-causal kernel-based approach (▮) closely approaches the perfect inverse-model feedforward P^{-1} (▮), whereas using only a causal kernel (▮) or none at all (▮) leads to deteriorated performance. The noise variance σ_y^2 is indicated by – –.

Monte Carlo simulations are performed for numerical illustration, with $m = 1000$ realizations. In each realization, two tasks are performed with $r(t)$ i.i.d. zero-mean normally distributed noise of length $N = 1000$ with variance $\sigma_r^2 = 1$.

- In the first task, the estimation data is generated according to $y(t) = P(q)r(t)$, where the measurement of $r(t)$ is contaminated with i.i.d. zero-mean normally distributed noise sequence $v_r(t)$ with variance $\sigma_v^2 = 1$, i.e., the SNR is $\sigma_r^2/\sigma_v^2 = 1$, see Figure 2b, and the inverse models are estimated in the backward setting.
- In the second task, the estimated inverse models $F(q, \hat{\theta})$ are used for feedforward as in Figure 1. That is, $y(t) = P(q)F(q, \hat{\theta})r(t) + v_y(t)$, where v_y is an i.i.d. zero-mean normally distributed noise sequence with variance $\sigma_y^2 = 1$, uncorrelated with r and v_r.

The obtained impulse responses from a single realization are shown in Figure 4, and a histogram of the resulting

two-norm of the tracking errors $e = r - y$ is depicted in Figure 5. The following observations are made:

- The perfect feedforward $F = P^{-1} = \sum_{k=-\infty}^{\infty} \theta_k^o z^{-k}$ enables optimal tracking performance $\bar{\mathbb{E}}\|e\|_2/\sqrt{N} = \sigma_y^2$. This confirms the validity of the non-causal interpretation of P^{-1}, see Section 3.
- The proposed kernel-based approach (6) with developed non-causal kernel (10) leads to high estimation accuracy and near-optimal feedforward performance.
- Not using regularization, i.e., (3), results in high variance of $\hat{\theta}$, and consequently poor performance.
- Using a pre-existing causal kernel leads to high variance of the non-regularized non-causal parameters, and hence moderate feedforward performance.

7. CONCLUSIONS

A kernel-based identification approach is developed to estimate non-causal models of inverse systems for feedforward control. The developed approach recovers and extends recent developments in kernel-based regularized identification, yet handles inverse systems with poles both inside and outside the usual stability region in a unified manner. This is enabled by using non-causal kernels, constructed using non-causal rational basis functions. Pre-existing kernel design choices, such as DC and TC, all fit into the developed framework. The effectiveness of the proposed approach is validated on an example system, including non-causality.

REFERENCES

Blanken, L., Isil, G., Koekebakker, S., and Oomen, T. (2018). Data-driven feedforward learning using non-causal rational basis functions: Application to an industrial flatbed printer. In *2018 IEEE American Control Conference*. Milwaukee, Wisconsin.

Boeren, F., Oomen, T., and Steinbuch, M. (2015). Iterative motion feedforward tuning: A data-driven approach based on instrumental variable identification. *Contr. Eng. Prac.*, 37, 11 – 19.

Bolder, J., Oomen, T., and Steinbuch, M. (2015). Rational basis functions in iterative learning control - with experimental verification on a motion system. *IEEE Trans. Contr. Syst. Technol.*, 23(2), 722–729.

Bolder, J., Kleinendorst, S., and Oomen, T. (2016). Data-driven multivariable ILC: enhanced performance by eliminating L and Q filters. *Int. J. Robust Nonlin.*

Butterworth, J., Pao, L., and Abramovitch, D. (2012). Analysis and comparison of three discrete-time feedforward model-inverse control techniques for nonminimum-phase systems. *Mechatronics*, 22(5), 577–587.

Chen, T., Ohlsson, H., and Ljung, L. (2012). On the estimation of transfer functions, regularizations and Gaussian processes-Revisited. *Automatica*, 48(8), 1525 – 1535.

Chen, T. and Ljung, L. (2015). Regularized system identification using orthonormal basis functions. In *Proceedings of the 2015 European Control Conference (ECC)*, 1291–1296. Linz, Austria.

Chen, T. and Francis, B.A. (1995). *Optimal Sampled-Data Control Systems*. Springer-Verlag, London, UK.

Darwish, M., Pillonetto, G., and Tóth, R. (2018). The quest for the right kernel in bayesian impulse response identification: the use of OBFs. *Automatica*, 87, 318 – 329.

Devasia, S. (1999). Approximated stable inversion for nonlinear systems with nonhyperbolic internal dynamics. *IEEE Transactions on Automatic Control*, 44(7), 1419–1425.

Gevers, M. (2005). Identification for control: From the early achievements to the revival of experiment design. *Eur. J. Control*, 11(4), 335 – 352.

Heuberger, P., Van den Hof, P., and Wahlberg, B. (2005). *Modelling and Identification with rational orthogonal basis functions*. Springer-Verlag, London, UK.

Jung, Y. and Enqvist, M. (2013). Estimating models of inverse systems. In *Proceedings of the 52nd IEEE Conference on Decision and Control*, 7143–7148. Florence, Italy.

Ljung, L. (1999). *System identification - Theory for the User*. Prentice-Hall, Upper Saddle River, NY, USA.

van den Meijdenberg, I. (2017). *Data-driven feedfoward control: a kernel-based estimation approach*. Master's thesis, Eindhoven University of Technology.

Middleton, R.H., Chen, J., and Freudenberg, J.S. (2004). Tracking sensitivity and achievable $\mathcal{H}_\infty$ performance in preview control. *Automatica*, 40(8), 1297–1306.

Ninness, B. and Gustafsson, F. (1997). A unifying construction of orthonormal bases for system identification. *IEEE Trans. Automat. Contr.*, 42(4), 515–521.

Ninness, B., Hjalmarsson, H., and Gustafsson, F. (1999). Generalized Fourier and Toeplitz results for rational orthonormal bases. *SIAM J. Control Optim*, 37(2), 429–460.

Pillonetto, G., Dinuzzo, F., Chen, T., De Nicolao, G., and Ljung, L. (2014). Kernel methods in system identification, machine learning and function estimation: A survey. *Automatica*, 50(3), 657 – 682.

Pillonetto, G. and Chiuso, A. (2015). Tuning complexity in regularized kernel-based regression and linear system identification. *Automatica*, 58(C), 106–117.

Pillonetto, G. and Nicolao, G.D. (2010). A new kernel-based approach for linear system identification. *Automatica*, 46(1), 81 – 93.

Rasmussen, C.E. and Williams, C.K.I. (2006). *Gaussian Processes for Machine Learning*. The MIT Press.

Söderström, T. (2002). *Discrete-time stochastic systems: estimation and control*. Springer, London, UK.

Söderström, T. and Stoica, P. (1989). *System identification*. Prentice Hall, Hemel Hempstead, U.K.

Vinnicombe, G. (2001). *Uncertainty and Feedback: $\mathcal{H}_\infty$ loop-shaping and the ν-gap metric*. Imperial College Press, London, U.K.

Zhou, K., Doyle, J., and Glover, K. (1996). *Robust and Optimal Control*. Prentice Hall, NJ.

van Zundert, J., Bolder, J., Koekebakker, S., and Oomen, T. (2016). Resource-efficient ILC for LTI/LTV systems through LQ tracking and stable inversion: Enabling large feedforward tasks on a position-dependent printer. *Mechatronics*, 38, 76 – 90.

van Zundert, J. and Oomen, T. (2017). On inversion-based approaches for feedforward and ILC. *IFAC Mechatronics*.